ELSEVIER

Polymer 44 (2003) 519–525

polymer

www.elsevier.com/locate/polymer

Simulation of GPC-distribution coefficients of linear and star-shaped molecules in spherical pores. 2. Comparison of simulation and experiment

Wolfgang Radke[a,*], Johannes Gerber[a], Gabriele Wittmann[b]

[a]*Deutsches Kunststoff-Institut, Schlossgartenstr. 6, Analytik, D-64289 Darmstadt, Germany*
[b]*Institut für Makromolekulare Chemie, Technische Universität Darmstadt, Petersenstr. 22, D-64287 Darmstadt, Germany*

Received 6 August 2002; received in revised form 29 October 2002; accepted 5 November 2002

Abstract

Star-polymers with arm numbers ranging from 3 to 10 have been synthesized and characterized by conventional GPC and GPC-light-scattering. The GPC elution behavior of the stars was studied and compared with predictions from computer simulations. The comparison of simulated and experimental data shows reasonable agreement if the arms are sufficiently long. Thus, using computer simulations GPC calibration curves of non-linear topologies can be constructed based on the calibration curve of the corresponding linear polymer. For star polymers prepared by atom transfer radical polymerization we found additional peaks having twice the molecular weight of the peak that has been assigned to the star. The elution volumes of these peaks were in good agreement with an expected dumbbell topology that would arise from coupling of the arms of different stars.

Keywords: GPC-distribution coefficients; Linear and star polymers; Atom transfer radical polymerization

1. Introduction

GPC is a major tool for polymer characterization. For linear chains a calibration curve is easily constructed by plotting the logarithm of molecular weight versus elution volume. For branched polymers, however, the situation is more complicated. Branched polymers exhibit a more dense structure than their linear analogues [1,2], resulting in a shift to higher elution volumes as compared to a linear molecule of the same chemical structure and molecular weight. The lack of polymer standards for branched polymers has lead to the frequent use of molecular weight sensitive detectors like on-line viscosity or on-line light-scattering detectors [3–7]. However, the high price of such instruments prevents the use of such instrumentation in every laboratory. Thus, it would be helpful if the elution volume of a branched polymer relative to the linear molecule could be predicted from theory or simulation.

In a recent publication [8] computer simulations have been used to show that the hydrodynamic radius calculated in the non-draining limit might serve as a universal parameter to determine the distribution coefficient of linear and star polymers in spherical pores. It was shown that the ratio of the molecular weights of linear and star-branched molecules having the same distribution coefficient only depends on the number of arms in the star polymer but not on its molecular weight. Thus, it should be possible to predict the GPC-elution behavior from computer simulation and the corresponding linear calibration curve.

The present article compares the results of the computer simulations with experimental data on the elution volume of star polymers of various numbers of arms and different arm lengths.

2. Experimental section

Simulations of self-avoiding walks in spherical pores were performed to calculate the distribution coefficients for linear and star-shaped structures. Details of the algorithm can be found elsewhere [8].

2.1. Synthesis of star polymers

Star polymers were synthesized by three different

* Corresponding author. Tel.: +49-6151162305; fax: +49-6151292855.
E-mail address: wradke@dki.tu-darmstadt.de (W. Radke).

0032-3861/03/$ - see front matter © 2002 Elsevier Science Ltd. All rights reserved.
PII: S0032-3861(02)00805-4

strategies. Two series were obtained by grafting narrow distributed living polystyrene (PS) anions onto narrow distributed poly(methyl methacrylate) (PMMA) standards of low molecular weight. Due to side reactions a large amount of residual precursor persists after the coupling reaction. Another series of PS stars was synthesized by crosslinking living polystyrene anions with divinylbenzene (DVB) in cyclohexane solution [9]. Due to the synthetic approaches used, the stars prepared were heterogeneous with respect to the number of arms, while the polydispersity of the arms was low. Gradient HPLC was used to fractionate the samples according to their number of arms. PS- and PMMA-stars with defined number of arms were synthesized by atom transfer radical polymerization (ATRP) using initiators with defined functionality. For these stars the number of arms is expected to be well defined [10]. However, no precursor, which allows the characterization of the molecular weight distribution of the arms, is available by this synthetic method. Finally additional PS-stars with 3, 4, 17 and 33 arms were gratefully obtained from PSS Polymer Standards Service GmbH, Mainz and Prof. Hirao, Tokyo Institute of Technology [11,12].

HPLC separations according to the number of arms were mostly performed on a modular HPLC system consisting of Shimadzu degasser DGU 14A, low pressure gradient former FCV10ALVp, HPLC-pump LC10ADVp, autosampler SIL10ADVp, Jetstream2 column oven, Thermo Separations UV2000 and PolymerLabs ELS1000 evaporative light-scattering detector. For data acquisition PSS WINGPC was used. Reversed phase-columns were used for the separations (Nucleosil, C18, 5 μm, 300 Å, 250 × 4.6 mm, Macherey & Nagel, Düren, Germany). Gradients were formed by acetonitrile/THF mixtures starting with a THF content of 35% and ending with a THF content of 51%. Gradient shapes were adjusted to the molecular weights of the arms in order to optimize separations.

2.2. Characterization

GPC analysis was performed in THF at a flow rate of 1 ml/min using a GPC equipped with Waters 510 pump, TSP AS100 autosampler, Waters 486 UV detector operated at 254 nm, Wyatt Technologies DAWN EOS light-scattering detector and Waters 410 RI-detector. A column set of three columns (PL-Gel mixed B, mixed C, mixed D 30 × 0.8 cm each) was used.

For conventional GPC experiments toluene was used as an internal flow marker, to correct for flow rate fluctuations. GPC-calibrations were performed using PS and PMMA standards (PSS Polymer Standards Service GmbH, Mainz, Germany). Data acquisition and evaluation was performed using PSS WINGPC Software (Version 4.12 and Version 6.2)

For data acquisition and evaluation of GPC light-scattering experiments Astra version 4.73 (Wyatt Technology, Santa Barbara, USA) was used. The light-scattering instrument was calibrated using pure toluene assuming Rayleigh ratio of $9.78 \times 10^{-6}\,\mathrm{cm}^{-1}$ at 690 nm. The injection volume of the fixed autosampler loop was determined gravimetrically to be 118 μl by filling the loop repeatedly with distilled water. For PMMA and PS refractive index increments of 0.089 and 0.184 cm^3/g at 633 nm were used [13], respectively, neglecting the 60 nm difference to the wavelength of the light-scattering instrument.

Typical sample concentrations for GPC-analysis were in the range of 0.5–5 g/l depending on molecular weight, polydispersity and scattering intensity. In crucial cases several concentrations were injected in order to control that overloading effects do not influence the results.

3. Results and discussion

3.1. Analysis of the GPC-elution behavior of star polymers

The star polymers synthesized by crosslinking or grafting reactions are heterogeneous with respect to the number of arms. GPC analysis of the crude reaction products showed only two peaks (Fig. 1). At high elution volumes (low molecular weights) terminated precursor can be identified in varying amounts, depending on the synthetic approach used. The amounts of residual precursor were generally lower for the crosslinking reactions than using the grafting approach. At low elution volumes (high molecular weights) peaks without any fine structure can be seen, which correspond to the expected stars.

Gradient HPLC was used to analytically separate stars of different functionality. Fig. 2 shows a typical separation by gradient chromatography of a star polymer. With increasing elution time the resolution of the different peaks becomes poorer. However, up to nine different species can be identified for an arm molecular weight of 11 000 g/mol. For

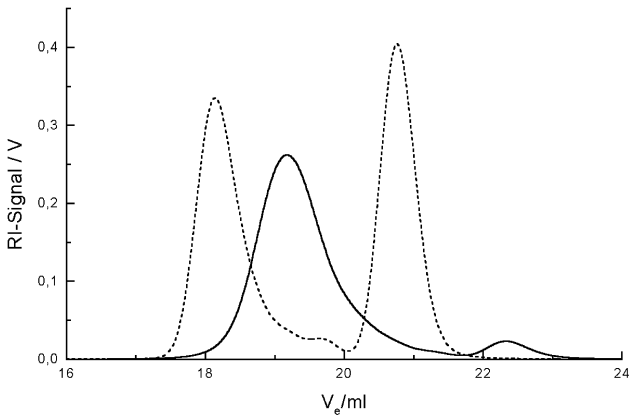

Fig. 1. Typical GPC-chromatograms of crude star polymers obtained by grafting linear PS onto narrow distributed low molecular weight PMMA (dotted line) or by crosslinking living PS chains with divinylbenzene (solid line).

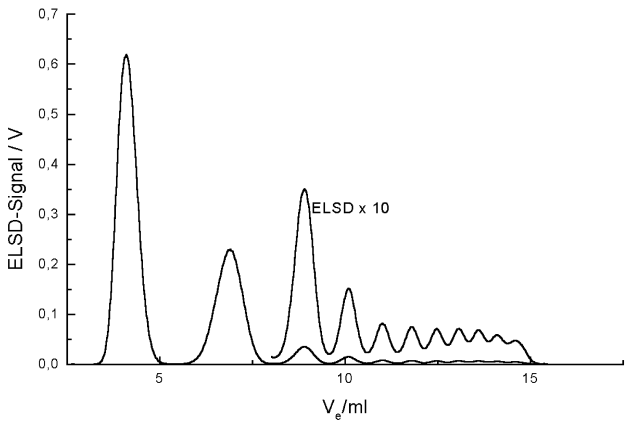

Fig. 2. Gradient HPLC separation of star polymers according to number of arms ($M_{peak,arm}$ = 11 300 g/mol).

lower molecular weight arms even higher number of species can be detected.

The different species were assumed to be star polymers having different numbers of arms. Multiple injections of the crude star mixtures allowed to collect fractions in amounts large enough for subsequent characterization by GPC and GPC-light-scattering and to analyze the elution behavior of the different stars. Fig. 3 shows a typical example of the GPC-light-scattering results of a fraction obtained. It becomes clear that the molecular weight is nearly constant throughout the peak resulting in a very low polydispersity. Fig. 4 shows the molecular weights at peak maximum of the RI-signal as a function of the fraction number. It can be seen that for the particular sample the molecular weight increases linearly by 11 000 g/mol for each fraction. This is exactly the molecular weight of the precursor which is identical to the first fraction. Thus, the different species can be assigned unambiguously to stars having different number of arms.

Knowing the molecular weight of the arm ($M_{peak,arm}$) and the number of arms, f, the molecular weight at peak maximum was calculated according to

$$M_{peak} = fM_{peak,arm} \quad (1)$$

The more appropriate way would be to use the number average molecular weights for the precursor and the star

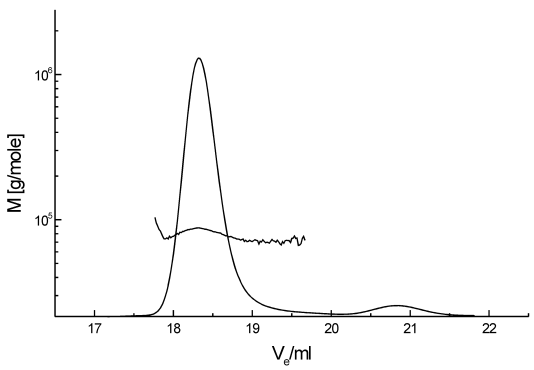

Fig. 3. GPC-light-scattering data of star fraction 8 ($M_{peak,arm}$ = 11 000 × g/mol, M_{peak} = 87 000 g/mol).

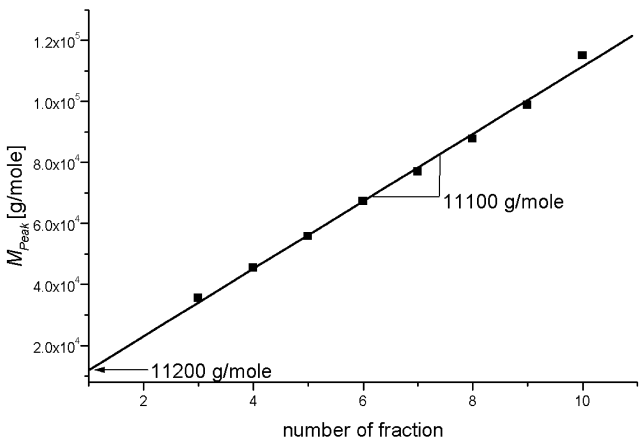

Fig. 4. Peak molecular weights of the star-fractions as function of the fraction number ($M_{peak,arm}$ = 11 300 g/mol).

polymer. The peak molecular weight of a star is not necessarily given by the approximation of Eq. (1). However, we have numerically calculated weight distributions for star polymers of various number of arms using the experimentally obtained weight distribution of the precursor. We found good agreement with Eq. (1) for the given distributions. This agreement is probably a consequence of the narrow and symmetrical molecular weight distribution of the precursor.

The true calibration curves for the star polymers, obtained by plotting log M_{peak} versus elution volume, are compared with the calibration curve for linear polystyrene in Fig. 5 (entries 14–43 in Table 1). This plot is very similar to Fig. 5 in Ref. [8]. The higher the number of arms for a particular arm length, the higher is the discrepancy between the true calibration and a calibration based on linear standards. The apparent molecular weight, which is obtained by applying a calibration curve constructed using linear standards of the same chemical structure as the star polymer, will be denoted $M_{peak,app}$.

Using computer simulations distribution coefficients, K, for linear and star-shaped polymers of different functionality

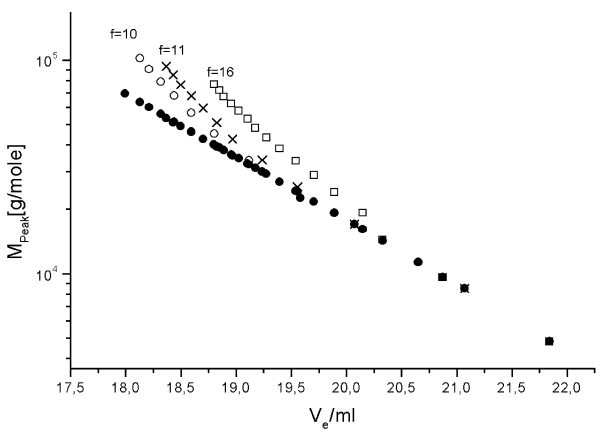

Fig. 5. Comparison of calibration curves for linear (●) and star polymers having arm length of $M_{peak,arm}$ = 4800 (□), 8500 (×) and 11 300 (○) g/mol.

Table 1
Comparison of γ-values for star polymers of different arm number, arm length and chemical structure

Entry	Polymer	f	γ_{exp}	γ_{sim}	M_{peak}	$M_{peak,arm}$
1	PS/ATRP	3	1.12	1.09	18 200	6000[a]
2	PMMA/ATRP	3	1.26	1.09	23 800	8000[a]
3	PS/ATRP	3	1.2	1.09	29 000	9800[a]
4	PS[b]	3	1.40	1.09	129 000[c]	45 500[d,c]
5	PMMA/ATRP	4	1.42	1.20	40 200	10 000[a]
6	PS/ATRP	4	1.29	1.20	44 000	11 000[a]
7	PS/ATRP	4	1.44	1.20	63 000	15 800[a]
8	PS/ATRP	8	1.48	1.64	59 400	7400[a]
9	PS[b]	8	1.80	1.64	425 000[c]	45 500[d,c]
10	PS[b]	17	1.99	2.52	87 600[c]	4900[e,c]
11	PS/DVB	18	2.52	2.61	610 000	34 000[f]
12	PS/DVB	21	2.73	2.86	462 000	22 000[f]
13	PS[b]	33	2.92	3.73	190 000[c]	5600[e,c]
14	PS/DVB	3	1.01	1.09	14 400	4800
15	PS/DVB	4	1.19	1.20	19 200	4800
16	PS/DVB	5	1.25	1.31	24 000	4800
17	PS/DVB	6	1.33	1.42	28 800	4800
18	PS/DVB	7	1.38	1.53	33 600	4800
19	PS/DVB	8	1.43	1.64	38 400	4800
20	PS/DVB	9	1.48	1.74	43 200	4800
21	PS/DVB	10	1.54	1.85	48 000	4800
22	PS/DVB	11	1.61	1.95	52 800	4800
23	PS/DVB	12	1.67	2.05	57 600	4800
24	PS/DVB	13	1.73	2.14	62 400	4800
25	PS/DVB	14	1.78	2.24	67 200	4800
26	PS/DVB	15	1.86	2.34	72 000	4800
27	PS/DVB	16	1.91	2.43	76 800	4800
28	PS/grafted	3	1.06	1.09	24 150	8500
29	PS/grafted	4	1.14	1.20	29 900	8500
30	PS/grafted	5	1.19	1.31	35 700	8500
31	PS/grafted	6	1.30	1.42	39 250	8500
32	PS/grafted	7	1.40	1.53	42 650	8500
33	PS/grafted	8	1.48	1.64	45 800	8500
34	PS/grafted	9	1.57	1.74	48 800	8500
35	PS/grafted	10	1.67	1.85	51 000	8500
36	PS/grafted	11	1.75	1.95	53 300	8500
37	PS/grafted	3	1.05	1.09	33 900	11 300
38	PS/grafted	4	1.13	1.20	45 200	11 300
39	PS/grafted	5	1.22	1.31	56 500	11 300
40	PS/grafted	6	1.32	1.42	67 800	11 300
41	PS/grafted	7	1.42	1.53	79 100	11 300
42	PS/grafted	8	1.51	1.64	90 400	11 300
43	PS/grafted	9	1.60	1.74	101 700	11 300
44	PS[b]	3.8	1.10	1.18	322 000	85 000[g]
45	PS[b]	4.2	1.13	1.23	358 000	85 000[g]
46	PS[b]	4.6	1.14	1.27	393 000	85 000[g]
47	PS[b]	4.9	1.19	1.31	420 000	85 000[g]
48	PS[b]	5.2	1.20	1.33	440 000	85 000[g]
49	PS[b]	5.3	1.23	1.35	454 000	85 000[g]
50	PSb	5.4	1.22	1.35	456 000	85 000[g]

[a] No precursor available, calculated using $M_{arm} = M_{peak}/f$.
[b] Well-defined linking agents.
[c] Information given by supplier.
[d] PSS Polymer Standards Service GmbH, Mainz, Germany.
[e] Prof. Akira Hirao, Tokyo Institute of Technology, Japan.
[f] Polydisperse samples, evaluation at peak maximum.
[g] M_n-data taken from Ref. [14].

and arm lengths were obtained for different pore sizes [8]. Comparing the number of segments of the linear, N_{lin}, and the star polymer, N_{star}, at the same value of K, we can define the ratio $\gamma_{sim} = N_{star}/N_{lin}$. This ratio gives the factor (according to the simulation) by which the molecular weight of a star is higher than obtained by using a calibration curve created with linear standards. The dependences of γ_{sim} on pore size and arm length are neglectable as long as our simulated polymers are far from the exclusion limit of the pore. The simulated data can be fitted by the following equation (Fig. 6):

$$\gamma_{sim} = 0.738 + 0.120f - 8.67 \times 10^{-4} f^2 \qquad 20 \geq f \geq 3 \quad (2)$$

Knowing the molecular weight of the precursor and assuming a functionality we can calculate the expected apparent molecular weight

$$M_{app}^{sim} = M_{peak}/\gamma_{sim} = f(M_{peak,arm}/\gamma_{sim}) \quad (3)$$

From the calibration curve of the corresponding linear polymer we can finally assign the elution volume corresponding to M_{app}^{sim} to the true molecular weight of the star polymer. The calibration curves constructed in this way were compared with the true calibration curves of the stars obtained experimentally and with the calibration curve of the linear polymer (Fig. 7).

From this figure it becomes clear that the true calibration curves differ substantially from the calibration curve constructed using linear standards. However, the simulation based calibration curves for arm lengths of 8300 and 11 300 g/mol (entries 28–43 in Table 1) are much closer to the true ones. For the lowest arm length (4800 g/mol, entries 14–27 in Table 1) the linear and the simulation based calibration curves strongly deviate from the true one.

This becomes even clearer in Fig. 8, which shows the errors in the molecular weights of the stars upon using a calibration based on linear standards or a simulation based calibration curve. Irrespective of the arm length the error associated with the use of a linear calibration curve reaches 40–50% as a function of the number of arms without reaching a limiting value. For arm lengths of 8300 and

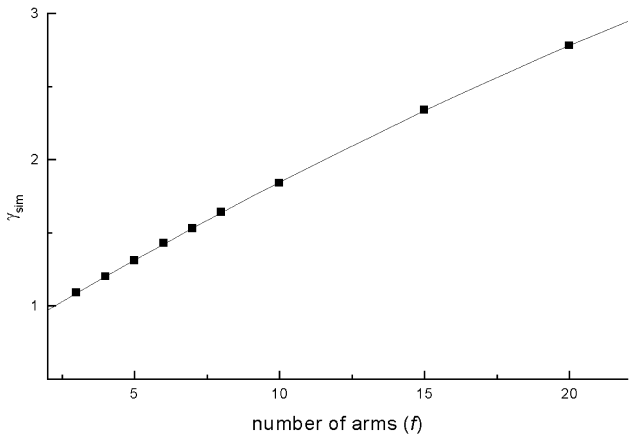

Fig. 6. Simulated values for γ_{sim} and fit according to Eq. (2).

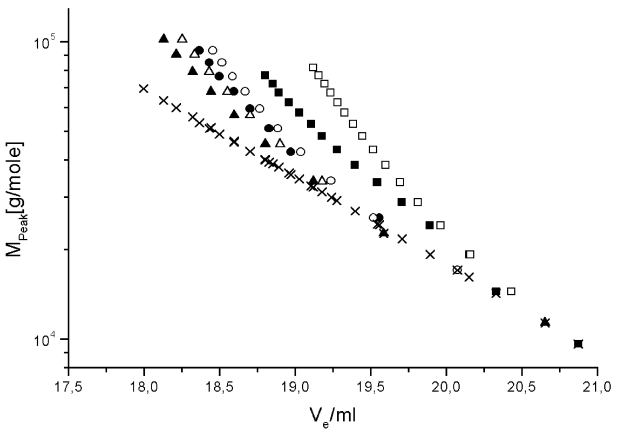

Fig. 7. True (solid symbols) and simulation based (open symbols) calibration curves for star polymers with an arm molecular weight of $M_{peak,arm}$ = 4800 (■□), 8500 (○●) and 11 300 (▲△) g/mol in comparison to a calibration curve constructed with linear standards (×).

11 300 g/mol (entries 28–43 in Table 1) the error between true and simulation based calibration reaches maximum values of 10–15%, while for stars having an arm length of 4800 g/mol (entries 14–27 in Table 1) a large overestimation of the molecular weights is observed when using the simulation based calibration curve i.e. for larger arm lengths the error associated with a simulation based calibration curve is about the same magnitude as the differences occurring normally between different methods of molecular weight determination. For the series having the shortest arm length, however, the molecular weights would be strongly overestimated by using the simulated data. Beside the lower molecular weight of the arms, these stars have been prepared by crosslinking with DVB. Thus, the chemical difference of the core might also be a reason for the deviation from the other experimental data points. We therefore analyzed two different star polymers prepared by crosslinking with DVB having arm length of $M_{peak,arm}$ = 22 000 and 34 000 g/mol (entries 11 and 12 in Table 1). For these polymers we have not yet been able to obtain a separation according to the number of arms using HPLC. Thus, GPC-light-scattering was used to determine the molecular weight at the peak maximum of the star. By taking the ratio $M_{peak}/M_{peak,arm}$ the number of arms at the peak maximum was determined experimentally to be 21 and 18, respectively. The apparent molecular weights were obtained from the GPC calibration curve and $\gamma_{exp} = M_{peak}/M_{app}$ was calculated. The corresponding number of arms was obtained from Eq. (2) to be 19 and 17, respectively. From the good agreement it seems as if the relatively low molecular weight of the arm and not the kind of coupling reaction is responsible for the stronger deviation. This interpretation is also confirmed by the results of star polymers from other sources (Table 1, Fig. 9). Here again the stars with low molecular weight arms show stronger deviations than stars having longer arms, as can be seen from Table 1 and Fig. 9.

Beside the effect of the low molecular weight arms it becomes apparent that for the samples which have been obtained by ATRP and from other sources the scattering of the data points is much higher than for the series obtained by separation using HPLC. This is mainly due to the characterization information that had to be combined from different sources. In some cases precursors have not been available in order to eliminate deviations of the GPC characterization of different laboratories. Further reason for the larger scattering is the fact that the majority of the stars have three and four arms. In that case the size reduction will lead only to small deviations between the true and the apparent molecular weights (10–20%). Thus, the error in molecular weight determination can easily exceed the effects of branching. However, we can conclude that for

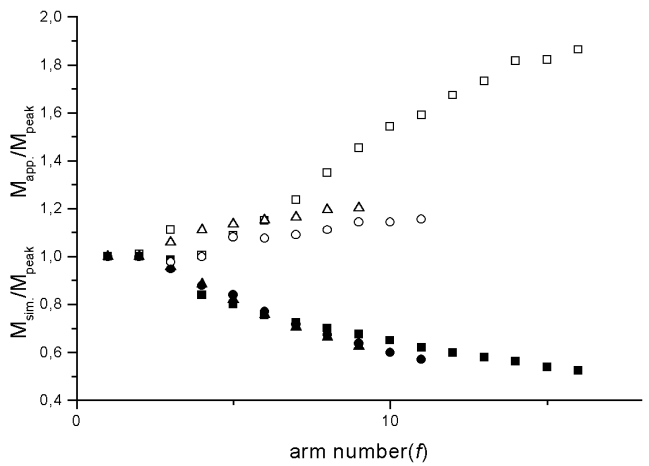

Fig. 8. Ratios of simulation based to true molecular weights (open symbols) and ratios of apparent to true molecular weights (solid symbols) as function of the number of arms ($M_{peak,arm}$ = 4800 (■□), 8500 (○●), 11 300 (▲△) g/mol).

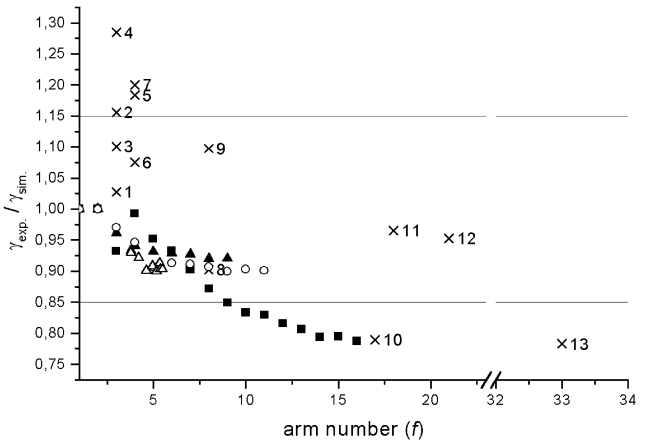

Fig. 9. Ratios $\gamma_{exp}/\gamma_{sim}$ as function of the number of arms for all samples investigated ($M_{peak,arm}$ = 4800 (■), 8500 (○), 11 300 (▲) g/mol, data taken from lit. [17] (△), others (×)). Lines denote 15% errors. The numbers correspond to the entries in Table 1.

high molecular weight arms we can predict the elution behavior of star polymers with reasonable accuracy.

Using the universal calibration approach results in the following equation for γ [15,16]

$$\gamma = g'^{(1/1+a)} \tag{4}$$

where g' is the ratio of the intrinsic viscosities of the branched and linear molecules taken at the same molecular weight, and a is the Mark–Houwink exponent of the linear polymer. For star polymers g' can be estimated from existing theories [17]. Thus, it is possible to calculate the calibration curve of the star polymer provided the Mark–Houwink exponent and g' is known. However, calculations of the intrinsic viscosities for branched structures are not trivial and thoroughly tested values for g' are available only for a small number of topologies. The simulation approach involves only the comparison of the molecular weights at the same value of the distribution coefficient. Thus, it can be easily extended to other topologies, for which no theoretical calculations of g' have been performed yet.

3.2. Structural elucidation of star polymers obtained by ATRP

For the star polymers obtained by ATRP the arm number is expected to be given by the functionality of the initiator moiety. However, no information on the molecular weight distribution of the arms is available.

In order to check whether the star polymers obtained by ATRP fit to the simulated data we determined the true and apparent molecular weight at peak maximum and calculated $\gamma_{exp} = M_{peak}/M_{app}$. These values were compared with the values expected from the functionality of the initiator and can be found in Table 1 and Fig. 9. For the given analysis we had to compare the data from GPC-light-scattering with GPC-data. Since even for polymer standards we find random deviations between molecular weights derived by the two methods in the order of 10%, the agreement between the γ-values found and expected from simulations is reasonable.

From inspection of the light-scattering traces it becomes apparent that the synthesis by ARTP is not free from side reactions. Figs. 10 and 11 show the RI- and 90°-light-scattering traces for typical star polymers obtained by ATRP. The RI-chromatogram of the three-arm star (Fig. 10) shows a shoulder at the high molecular weight side, while the light-scattering signal shows a pronounced signal in the high molecular weight region. The light-scattering analysis yields a molecular weight of 28 600 g/mol and $\gamma_{exp} = 1.2$ for the peak maximum of the RI (Table 1). For the peak maximum of the light-scattering signal we obtain a molecular weight of approximately 54 000 g/mol and $\gamma_{exp} = 1.12$. Thus, the molecular weight of the unknown second peak is about twice the molecular weight of the first peak and a coupling reaction seems plausible. Similar observations have been described in literature for ATRP as

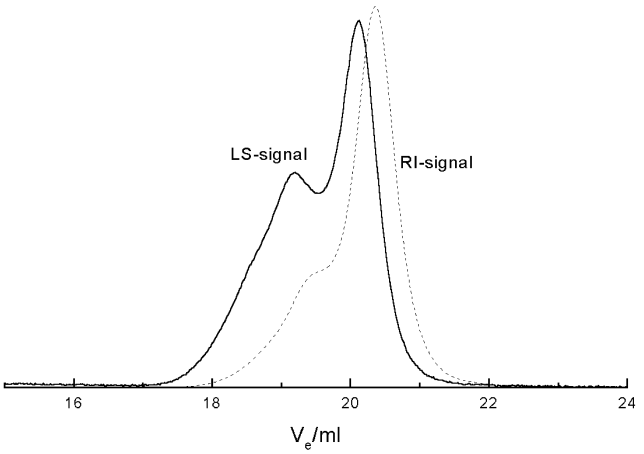

Fig. 10. RI (dotted curve) and 90°LS-trace (solid curve) for three-arm star polymer obtained by ATRP.

well as for stars synthesized by anionic polymerization [10,18,19]. The combination of two living radicals at the growing arms of different stars should result in a dumbbell-topology (Scheme 1) with the distance between the two branch points being twice the molecular weight of an arm (provided coupling occurs when nearly all monomer has been consumed). For this structure we performed computer simulations similar to those for the stars. We obtained a value of $\gamma_{sim} = 1.10$ for a branch point functionality of 3. The value found experimentally ($\gamma_{exp} = 1.12$) therefore perfectly fits this picture.

As another example for side reactions occurring in ATRP the RI and light-scattering traces of an eight-arm star are shown in Fig. 11. Clearly three different peak maxima can be distinguished. The molecular weights obtained are 15 000, 58 800 and 111 000 g/mol, while the γ-values found are $\gamma_{exp} = 1.06$, 1.53 and 1.90, respectively. For the eight-arm star a value of $\gamma_{exp} = 1.06$, is much too low (expected $\gamma_{exp} = 1.64$,). Comparing the molecular weights of the first and second peak we realize that the molecular weight of the second peak is approximately four times the molecular weight of the first one. The synthesis of the

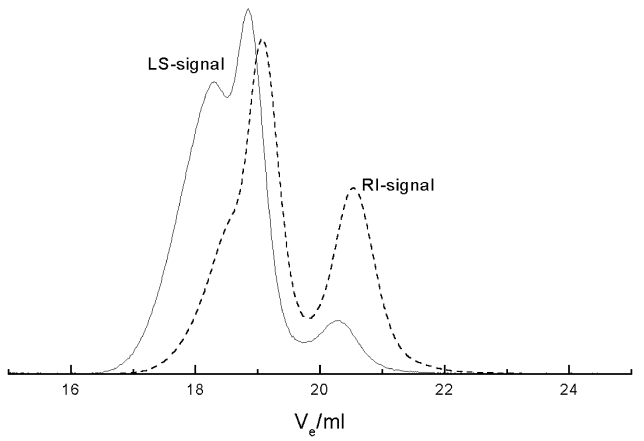

Fig. 11. RI (dotted curve) and 90°LS-trace (solid curve) for eight-arm star polymer obtained by ATRP.

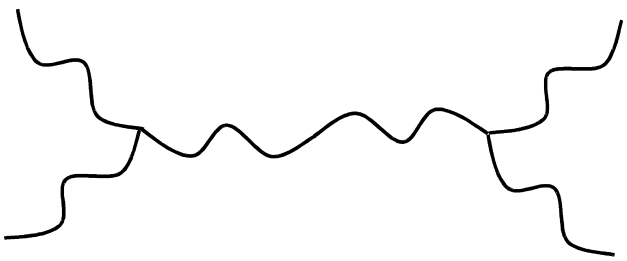

Scheme 1. Dumbbell topology resulting from coupling of three-arm stars.

octafunctional initiator involves the tetrafunctional coupling reaction of bifunctional initiator moieties (Scheme 2). Therefore, it is reasonable to assume that the first peak originates from bifunctional initiator residues due to insufficient purification of the octafunctional initiator. The second peak is the expected eight-arm star. This is in agreement with the γ-value found ($\gamma_{exp} = 1.53$, $\gamma_{sim} = 1.64$). The third peak, which is clearly visible in the light-scattering trace has about twice the molecular weight of the star and might be attributed again to the dumbbell structure resulting from the coupling reaction of two eight-arm stars. From simulation we expect for this kind of dumbbell $\gamma_{sim} = 1.79$, which corresponds well with the value found ($\gamma_{exp} = 1.90$). It should be noted that the peak maxima of the light-scattering peaks are not necessarily the true peak maxima for the respective structures, which will therefore influence the agreement between simulation and experiment.

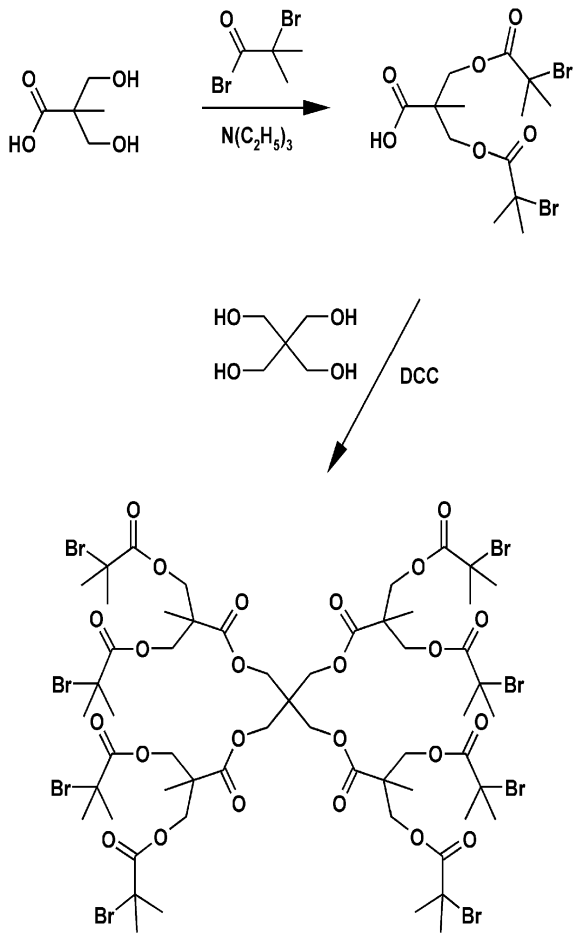

Scheme 2. Synthesis of octafunctional initiator for ATRP.

4. Conclusions

It was shown that it is possible to construct calibration curves for star polymers based on simulations and the calibration curve of the linear polymer provided the molecular weight are sufficiently high. Thus, for high molecular weight branched polymers computer simulations can help to obtain calibration curves for branched materials for which no standards are available. Furthermore the γ-values can be used in order to elucidate unknown structures. For stars synthesized by ATRP coupling reactions occur. The γ-values for these structures fit with the assumption of a dumbbell like and not for a star like coupling product.

Acknowledgements

The authors would like to express their gratitude to Prof. A. Hirao, Tokyo Institute of Technology and PSS Polymer Standards Service GmbH, Mainz for supplying samples. Part of this work was financially supported by the Deutsche Forschungsgemeinschaft (grant Ra 952/1-1)

References

[1] Zimm BH, Stockmayer WH. J Chem Phys 1949;17:1301.
[2] Casassa EF, Tagami Y. Macromolecules 1969;2:14.
[3] Haney MA. J Appl Polym Sci 1985;30:3037.
[4] Haney MA. J Appl Polym Sci 1985;30:3023.
[5] Haney MA. American Laboratory; 1985.
[6] Wyatt PJ. Anal Chim Acta 1994;677:21.
[7] Yau WW. Chemtracts, Macromol Chem 1990;1:1.
[8] Radke W. Macromol Theory Simul 2001;10:668.
[9] Tsistilianis C, Papanagopouls D, Lutz P. Polymer 1995;36:3745.
[10] Matyjaszewski K, Miller PJ, Pyun J, Kickelbick G, Diamanti S. Macromolecules 1999;32:6526.
[11] Hirao A. Presented at the International Symposium on Ionic Polymerization; Crete Oct 2001.
[12] Hirao A, Hayashi M, Haraguchi N. Macromol Rapid Commun 2000; 21:1171.
[13] Berkowitz SA. J Liq Chromatogr 1983;6:1359.
[14] Chang T, Lee HC, Lee W, Park S, Ko C. Macromol Chem Phys 1999; 200:2188.
[15] Strazielle C, Herz J. Eur Polym J 1977;13:223.
[16] Tsitsilianis C, Ktoridis A. Macromol Rapid Commun 1994;15:845.
[17] Roovers J. Dilute solution properties of regular star polymers. In: Mishra MK, Kobayashi S, editors. Star and hyperbranched polymers. New York: Marcel Dekker; 1999. p. 308–14.
[18] Angot S, Muthy KS, Taton D, Gnanou Y. Macromolecules 1998;31: 7218.
[19] Frater DJ, Mays JW, Jackson C. J Polym Sci, Part B: Polym Phys 1997;35:141.